

- [4] a) C. M. Carr, P. S. Kim, *Cell* **1993**, 73, 823–832; b) J. M. White, I. A. Wilson, *J. Cell Biol.* **1987**, 105, 2887–2896; c) L. H. Pinto, L. J. Holsinger, R. A. Lamb, *Cell* **1992**, 69, 517–528.
- [5] a) *Neoglycoconjugates: Preparation and Applications* (Eds.: Y. C. Lee, R. T. Lee), Academic Press, San Diego, CA, **1994**; b) Y. C. Lee, R. T. Lee, *J. Biomed. Sci.* **1996**, 3, 221–237; c) R. Roy, *Trends Glycosci. Glycotechnol.* **1996**, 8, 79–99; d) M. Mammen, G. Dahmann, G. M. Whitesides, *J. Med. Chem.* **1995**, 38, 4179–4190.
- [6] a) K. Nagata, T. Furuike, S.-I. Nishimura, *J. Biochem.* **1995**, 118, 278–284; b) W. Spevak, C. Foxall, D. H. Charych, F. Dasgupta, J. O. Nagy, *J. Med. Chem.* **1996**, 39, 1018–1020; c) K. Akiyoshi, J. Sunamoto, *Supramol. Sci.* **1996**, 3, 157–163; d) K. H. Mortell, R. V. Weatherman, L. L. Kiessling, *J. Am. Chem. Soc.* **1996**, 118, 2297–2298; e) K. Kobayashi, A. Tsuchida, *Macromolecules* **1997**, 30, 2016–2020; f) P. Arya, S. Dion, G. K. H. Shimizu, *Bioorg. Med. Chem. Lett.* **1997**, 7, 1537–1542; g) G. Thoma, B. Ernst, F. Schwarzenbach, R. O. Duthaler, *ibid.* **1997**, 7, 1705–1708.
- [7] a) M. N. Matrosovich, L. V. Mochalova, V. P. Marinina, N. E. Byramova, N. V. Bovin, *FEBS Lett.* **1990**, 272, 209–212; b) A. Gamian, M. Chomik, C. A. Laferrière, R. Roy, *Can. J. Microbiol.* **1991**, 37, 233–237; c) A. Spaltenstein, G. M. Whitesides, *J. Am. Chem. Soc.* **1991**, 113, 686–687; d) J. O. Nagy, P. Wang, J. H. Gilbert, M. E. Schaefer, T. G. Hill, M. R. Callstrom, M. D. Bednarski, *J. Med. Chem.* **1992**, 35, 4501–4502; e) S. Sabesan, J. Ø. Duus, S. Neira, P. Domaille, S. Kelm, J. C. Paulson, K. Bock, *J. Am. Chem. Soc.* **1992**, 114, 8363–8375; f) S.-I. Nishimura, K. B. Lee, K. Matsuoka, Y. C. Lee, *Biochem. Biophys. Res. Commun.* **1994**, 199, 249–254; g) W. J. Lee, A. Spaltenstein, J. E. Kingery-Wood, G. M. Whitesides, *J. Med. Chem.* **1994**, 37, 3419–3433; h) M. Itoh, P. Hetterich, R. Isecke, R. Brossmer, H.-D. Klenk, *Virology* **1995**, 212, 340–347; i) S. Cao, R. Roy, *Tetrahedron Lett.* **1996**, 37, 3421–3424; j) G. B. Sigal, M. Mammen, G. Dahmann, G. M. Whitesides, *J. Am. Chem. Soc.* **1996**, 118, 3789–3800; k) D. Zanini, R. Roy, *ibid.* **1997**, 119, 2088–2095; l) A. S. Gambaryan, A. B. Tuzikov, V. E. Piskarev, S. S. Yamnikova, D. K. Lvov, J. S. Robertson, N. V. Bovin, M. N. Matrosovich, *Virology* **1997**, 232, 345–350.
- [8] a) C. Unverzagt, S. Kelm, J. C. Paulson, *Carbohydr. Res.* **1994**, 251, 285–301, and references therein; b) H. Paulsen, S. Peters, T. Biefeldt, M. Meldal, K. Bock, *ibid.* **1995**, 268, 17–34; c) U. Sprengard, M. Schudok, W. Schmidt, G. Kretzschmar, H. Kunz, *Angew. Chem.* **1996**, 108, 359–362; *Angew. Chem. Int. Ed. Engl.* **1996**, 35, 321–324.
- [9] a) K. Aoi, H. Itoh, M. Okada, *Macromolecules* **1995**, 28, 5391–5393; b) T. K. Lindhorst, C. Kieburg, *Angew. Chem.* **1996**, 108, 2083–2086; *Angew. Chem. Int. Ed. Engl.* **1996**, 35, 1953–1956; c) P. R. Ashton, S. E. Boyd, C. L. Brown, N. Jayaraman, J. F. Stoddart, *ibid.* **1997**, 109, 756–759 and **1997**, 36, 732–735.
- [10] a) T. Toyokuni, B. Dean, S. Cai, D. Boivin, S.-I. Hakimori, A. K. Singhal, *J. Am. Chem. Soc.* **1994**, 116, 395–396; b) C.-C. Lin, T. Kimura, S. H. Wu, G. Weitz-Schmidt, C.-H. Wong, *Bioorg. Med. Chem. Lett.* **1996**, 6, 2755–2760; c) Y. Okumura, J. Sunamoto, *Supramol. Sci.* **1996**, 3, 171–176; d) M. Koketsu, T. Nitoda, H. Sugino, L. R. Juneja, M. Kim, T. Yamamoto, C.-H. Wong, *J. Med. Chem.* **1997**, 40, 3332–3335; e) T. Murohara, J. Margiotta, L. M. Phillips, J. C. Paulson, S. DeFrees, S. Zalipsky, L. S. S. Guo, A. M. Lefer, *Cardiovasc. Res.* **1997**, 30, 965–974.
- [11] A. Hasegawa, N. Suzuki, F. Kozawa, H. Ishida, M. Kiso, *J. Carbohydr. Chem.* **1996**, 15, 639–648.
- [12] H. Hirabayashi, M. Nishikawa, Y. Takakura, M. Hashida, *Pharm. Res.* **1996**, 13, 880–884.
- [13] R. P. Haugland in *Molecular Probes* (Ed.: M. T. Z. Spence), Molecular Probes, Eugene, OR, USA, **1992**.
- [14]  $R_f = 0.27$  ( $\text{CHCl}_3/\text{CH}_3\text{OH}/15\text{ mM CaCl}_2$  (60/35/8, v/v/v),  $^1\text{H}$  NMR (600 MHz,  $\text{CD}_3\text{OD}$ ):  $\delta = 7.34$  (s, 1H, BODIPY), 6.93 (d, 1H, BODIPY), 6.26 (d, 1H, BODIPY), 6.13 (s, 1H, BODIPY), 3.13 (m, 2H, BODIPY- $\text{CH}_2$ ), 2.62 (t, 2H, BODIPY- $\text{CH}_2$ ), 2.42 (s, 3H, BODIPY- $\text{CH}_3$ ), 2.19 (s, 3H, BODIPY- $\text{CH}_3$ ), 4.2–4.3 (1H,  $\text{C}_a\text{-H}$ ), 3.03 (m, 2H,  $\text{C}_\beta\text{-H}$ ), 1.5–1.65 (m, 4H,  $\text{C}_\beta\text{-H}$ ,  $\text{C}_\gamma\text{-H}$ ), 1.69 (m, 2H,  $\text{C}_\delta\text{-H}$ ), 4.21 (d, 1H,  $J = 8.1$  Hz, Glc-H1), 4.32 (d, 1H,  $J = 8.1$  Hz, Gal-H1), 3.93–3.95 (1H, Gal-H3), 3.80 (br. s, 1H, Gal-H4), 2.81 (dd, 1H, Neu5Ac-H3<sub>eq</sub>), 1.54 (1H, Neu5Ac-H3<sub>ax</sub>), 1.91 (3H, Neu5Ac-NHCOCH<sub>3</sub>), 5.32–5.38 (m, 1H, sphingosine, olefinic H4), 5.56–5.59 (m, 1H, sphingosine, olefinic H5), 1.19 (16H, sphingosine- $\text{CH}_2$ ), 0.80 (sphingosine- $\text{CH}_3$ ); ESI-MS positive ions: calcd for  $[\text{M}2\text{Na} - \text{H}]^+$ : 1362, found: 1362; calcd for  $[\text{M} + \text{Na}]^+$ : 1340, found: 1340; negative ions: calcd for  $[\text{M} - \text{H}]^-$ : 1316, found 1316.
- [15] The average molecular weight ( $\bar{M}_n$ ) was estimated to be 87 kDa based on the lyso-GM<sub>3</sub> content (0.72%;  $m = 536.1$ ,  $n = 3.9$ ) and the degree of polymerization ( $\text{DP} = 540$ ) of PGA.  $\bar{M}_n$  of **9** estimated by GPC to be 336 kDa (Waters Ultrahydrogel Liner column (7.8 × 300 mm), elution with 0.1 M  $\text{NaNO}_3$ , flow rate 1 mL min<sup>-1</sup>, UV detection at 500 nm and 40°C). Millenium 2010 with GPC software was used to analyze the data. Polyethylene oxides were employed as standards and detected by refractive index. The GPC result is apparently erroneous with respect to the number of introduced lyso-GM<sub>3</sub> groups ( $\bar{M}_n(\text{GPC})/\bar{M}_n(\text{UV}) = 3.86$ ), perhaps as a result of aggregation.
- [16] The inhibitory activity of polymer **9** toward influenza virus A/PR/8/34 (H1N1) was determined with an ELISA. Thus, an ethanol solution with 1 nmol of GM<sub>3</sub> was added to each well of 96-microwell plates. The solvent was evaporated at 37°C, and the remaining binding sites on the wells were blocked for 12 h at 4°C with 200  $\mu\text{L}$  of phosphate-buffered saline (PBS; 0.15 M NaCl, 8.1 mM  $\text{Na}_2\text{HPO}_4$ , 1.5 mM  $\text{NaH}_2\text{PO}_4$ ) that contained 2% bovine serum albumin (BSA). The wells were then washed five times with PBS. A series of dilutions, each by a factor of two, was prepared from a solution of the polymer (200 pmol) in 0.2% BSA-PBS. These dilute solutions were preincubated at 4°C for 2 h with 50  $\mu\text{L}$  of the influenza virus suspension (32 hemagglutinin units (HAU) and then introduced into the wells. The plates were incubated at 4°C for 12 h, washed five times with PBS, and then incubated for 2 h at 4°C with a 1000-fold diluted 0.2% BSA-PBS solution of 50  $\mu\text{L}$  of anti-influenza virus antibodies and treated at 4°C for 2 h with horse radish peroxidase (HRP)-conjugated protein A diluted 1000-fold with solution A. The virions bound to GM<sub>3</sub> and immobilized in the wells were detected with *o*-phenylenediamine (OPD) solution that contained 4 mg of OPD and 0.01%  $\text{H}_2\text{O}_2$  in 100 mM of phosphate buffer (adjusted to pH 5.0 with citric acid). The reactions were terminated by addition of 4 N  $\text{H}_2\text{SO}_4$ , and viral binding activities in the form of color development were determined at 492 nm (reference wavelength 630 nm). Serial dilutions (dilution factor two) of sialyl lactose (2  $\mu\text{mol}$ ), PGA (800 pmol), and lyso-GM<sub>3</sub> (20 nmol) were tested as controls in the manner described.
- [17] The HA trimer of H1 serotype influenza virus contains a total of 15 Trp residues.

## Assembly of DNA/Fullerene Hybrid Materials\*\*

Alan M. Cassell, Walter A. Scrivens, and James M. Tour\*

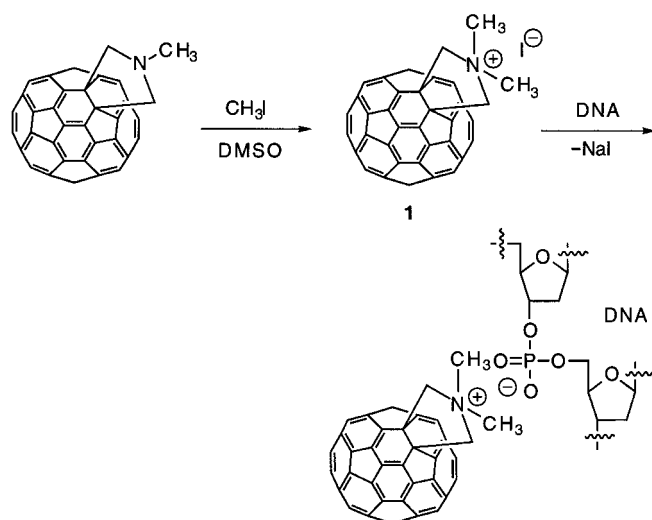
There are biochemical approaches to molecular structures of precisely defined dimensions ranging from 1 nm to 10  $\mu\text{m}$  in length. Conversely, the synthesis of precisely defined unnatural molecular architectures beyond 25 nm in length is often unattainable due to solubility, material through-put, and characterization constraints.<sup>[1]</sup> Therefore, as nanotechnological needs advance, syntheses could rely upon self-assembling strategies using natural scaffolds as templates for the construction of synthetic nanostructures.<sup>[2]</sup> DNA is particularly

[\*] Prof. J. M. Tour, Dr. A. M. Cassell, Dr. W. A. Scrivens  
Department of Chemistry and Biochemistry  
University of South Carolina  
Columbia, SC 29208 (USA)  
Fax: (+1) 803-777-9521  
E-mail: tour@psc.sc.edu

[\*\*] This research work was supported by the Defense Advanced Research Projects Agency and the Office of Naval Research.

well-suited for use as a molecular-based scaffold due to its structural regularity, its ability to reversibly assemble through hydrogen bonding, and the relative ease in obtaining materials of precise length well beyond the 25 nm regime. Most studies involving DNA self-assembly have focused on the duplex interactions between complementary DNA strands, the insertion of synthetic units through covalent tethering to specific nucleotides, or intercalation strategies. There are fewer studies involving the assembly of materials through electrostatic interactions on the phosphate groups along a DNA backbone.<sup>[3]</sup> We sought to exploit these successive negatively charged groups to rapidly assemble cationic molecules along the exterior of a DNA template. Furthermore, the analysis of large nanostructured materials is often tedious. A notable exception is seen with carbon nanotubes where transmission electron microscopy (TEM) provides high-contrast images without the need for heavy-metal coating or staining (which can severely inhibit resolution).<sup>[4]</sup> Thus, fullerene derivatives<sup>[5]</sup> were chosen as the DNA complexing agents, and we report here a new and facile route to nanostructures constructed from DNA/fullerene hybrids that can be rapidly imaged using TEM.

*C*<sub>60</sub>-*N,N*-Dimethylpyrrolidinium iodide (**1**) was synthesized to serve as the complexing agent (Scheme 1).<sup>[6]</sup> Molecular



Scheme 1. DNA is complexed by cation exchange of compound **1** with DNA.

modeling indicated that the complexation of **1'** (the iodide-free fullerene) along successive phosphate groups of a DNA backbone is sterically permitted (Figure 1) and that the thickness of the double-stranded DNA/**1'** complex would be 5–6 nm. DNA/**1'** complexes were then prepared by mixing the DNA solution with a solution of **1** in dimethyl sulfoxide. Indeed, the hybrid DNA/fullerene-based nanoarchitectures were easily imaged by TEM without heavy metal. Figure 2 shows the excellent contrast that was obtained between the complexed DNA and the carbon-film background.

Initially, the vast amount of aggregation (and possible supercoiling) hindered us from measuring the length and diameter of individual plasmids. We suspected that the enhanced aggregation arose in part from favorable van der Waals interactions between the hydrophobic portions of the

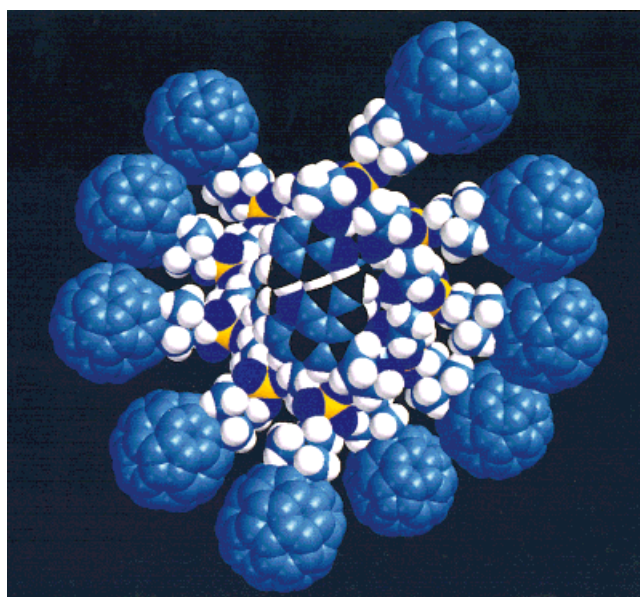


Figure 1. End-on view of the space-filling model of the CG duplex hexamer of DNA complexed with **1'**. Molecular modeling was performed with a Silicon Graphics Power Indigo2 work station employing MacroModel 4.5 for both structure drawing and energy minimization. Energy minimization of **1** was conducted with the MM2\* force field, and energy minimization of oligonucleotides was conducted with the AMBER\* force field. A third energy minimization calculation was then performed on the complex using the MM2\* force field. All energy calculations were minimized over a large number of iterations to convergence at the local minima nearest in energy to the initial energies of the starting compounds.

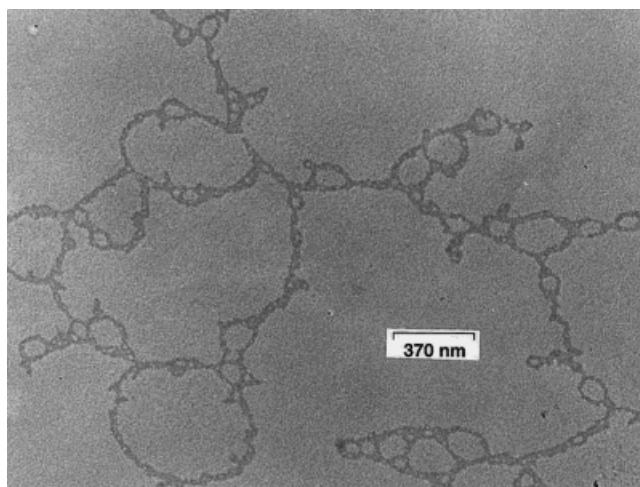


Figure 2. A solution of plasmid DNA ( $\phi$ X174RFII, a popular electron microscopy standard, prerelaxed plasmid, 5386 bp, 10  $\mu\text{g mL}^{-1}$ , 10 mM Tris-HCl, pH 8.5) was mixed with a solution of *C*<sub>60</sub>-*N,N*-dimethylpyrrolidinium iodide (5 mM in dimethyl sulfoxide, 150 equivalents of **1** per base) by gently shaking the mixture. After 4 h, 10  $\mu\text{L}$  of the DNA/**1'** complex solution was placed on a microscope slide positioned in a petri dish that contained distilled water. The solution traveled down the slide and spread as it contacted the water surface. A carbon-film coated TEM grid was then streaked across the top of the water, and the DNA/**1'** complexes were absorbed. The grid was wicked dry with a piece of filter paper, and placed under vacuum at 30°C for 1 h. The grid was placed in a Hitachi H-8000 electron microscope and imaged at 100 kV accelerating voltage.

fullerenes once the complexes were spread on water. We then screened a series of surfactants for their ability to lessen the fullerene attractive interactions in the DNA/**1'** complexes.

Surfactants were chosen that would not undergo cation exchange with the DNA/**1** complexes, for example, anionic, neutral, or zwitterionic surfactants. The surfactants were added to the water surface before the DNA/**1** complex solution (10  $\mu$ L). A neutral surfactant, Tween 20<sup>[7]</sup> (a trihydroxyl-terminated oligoether), did not change the previously observed structure of the DNA/**1** complexes imaged by TEM; they remained highly aggregated. Coco Betaine ((Me<sub>3</sub>SiO)<sub>2</sub>MeSiO(CH<sub>2</sub>CH<sub>2</sub>O)<sub>n</sub>H) kept the DNA/**1** complexes segregated, but they remained condensed (compacted) and highly supercoiled. The best results were obtained with Zonyl (CF<sub>3</sub>(CF<sub>2</sub>)<sub>8</sub>CO<sub>2</sub>Na), Admox 12 (CH<sub>3</sub>(CH<sub>2</sub>)<sub>11</sub>N(CH<sub>3</sub>)<sub>2</sub>O), and Admox 14 (CH<sub>3</sub>(CH<sub>2</sub>)<sub>13</sub>N(CH<sub>3</sub>)<sub>2</sub>O). Each of these surfactants availed segregated complexes. Instead of being completely aggregated (as in Figure 2), the complexes were in a condensed form in which the plasmids retained a contorted circular shape (Figure 3). Interestingly, the measured strand

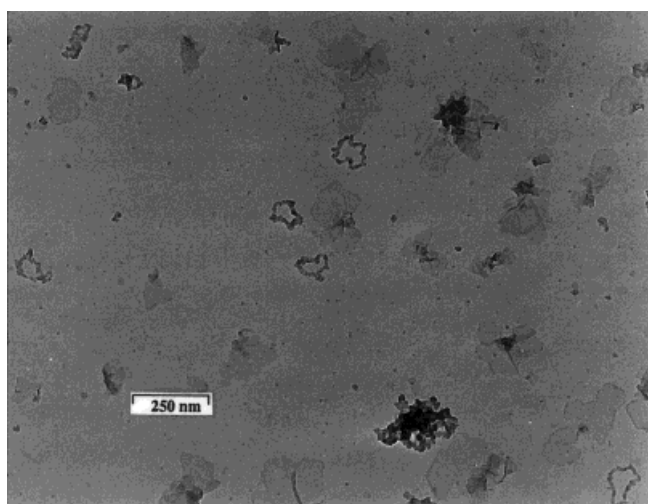


Figure 3. Image of condensed plasmid DNA (same as used for Figure 2) spread in the presence of Admox 14 (10  $\mu$ M). The other structures could be salts such as surfactant aggregates with **1** or Tris-HCl.

thicknesses of the plasmids in Figure 3 ranged between 15 and 30 nm. While the diameters of the DNA/**1** rings in Figure 3 ranged between 100 and 150 nm, the diameters of the prerelaxed plasmid DNA should be 580 nm if no condensation occurs;<sup>[8]</sup> the measured diameter was therefore 1/4–1/6 the expected diameter. Although bacterial DNA does not

have histones, this condensed state is noteworthy since it is reminiscent of DNA packing by histones in chromatin where the typical diameters of the solenoid are 30 nm.<sup>[9]</sup> The same effect was seen when we subjected linear DNA/**1** complexes to the surfactant series; again a condensed linear complex formed (Figure 4). The measured length of the

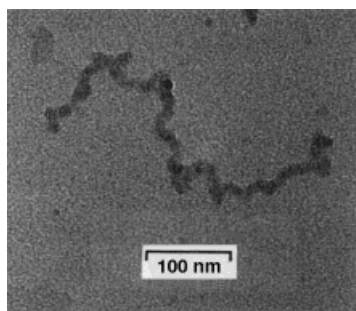


Figure 4. Image of condensed linear DNA (5686 bp, 1.93  $\mu$ m B-form length) spread in the presence of Admox 14 (10  $\mu$ M).

linear DNA/**1** complex is approximately 0.88  $\mu$ m, while its expected length is 1.93  $\mu$ m. The condensation is likely due to an intramolecular attraction of the fullerenes. We suspect the surfactant permits well-segregated DNA/**1** structures on water, thereby making the nonaggregated species abundant.

For the control experiments, we were unable to image DNA mixed with surfactants in the absence of **1**. Therefore, the surfactants do not complex with the DNA, or they do not provide enough electron density for imaging by TEM. Additionally, the use of **1** (or **1**/surfactant) without DNA does not afford these controlled nanostructures.

Although complexation of all the phosphates groups is sterically permitted (vide supra), the actual degree of substitution could not be assessed. Exhaustive substitution is unlikely, but the dramatic condensation insures sufficient fullerene density to permit contiguous imaging of the structure.

Use of a ferrocene-derived ammonium salt<sup>[10]</sup> instead of **1** resulted in image contrast inferior to that obtained from the DNA/**1** complexes. Therefore, in spite of the metal atoms in the ferrocene salts, fullerenes remained superior as contrast agents.

DNA can be used as a framework for the assembly of fullerene materials through electrostatic interactions with the phosphate groups along the DNA backbone. Since exhaustive substitution on the phosphate moieties could not be verified, the DNA/fullerene complexes described here are not assured of a precise structure. However, this method provides a rapid one-step route to hybrid nanoarchitectures in size regimes inaccessible by traditional synthetic methods; therefore, this and analogous DNA-templating routes may prove to be of enormous utility. While we anticipate that complexation of other cationic species will also yield well-ordered nanostructures, fullerenes provide the necessary imaging contrast for TEM analysis. Further work to intramolecularly cross-link the fullerenes along the DNA backbones would provide a route to more rigid polyfullerenes.

Received: November 10, 1997

Revised version: February 12, 1998 [Z11137IE]

German version: *Angew. Chem.* **1998**, *110*, 1670–1672

**Keywords:** DNA structures • fullerenes • nanostructures

- [1] J. M. Tour, *Chem. Rev.* **1996**, *96*, 537–553; b) G. M. Whitesides, J. P. Mathias, C. T. Seto, *Science* **1991**, *254*, 1312–1319.
- [2] a) C. M. Niemeyer; *Angew. Chem.* **1997**, *109*, 603–606; *Angew. Chem. Int. Ed. Engl.* **1997**, *36*, 585–587; b) C. A. Mirkin, R. L. Letsinger, R. C. Mucic, J. J. Storhoff, *Nature* **1996**, *382*, 607–609; c) A. P. Alivisatos, K. P. Johnsson, X. Peng, T. E. Wilson, C. J. Loweth, M. P. Bruchez, P. G. Schultz, *Nature* **1996**, *382*, 609–611; d) J. Chen, N. C. Seeman, *Nature* **1991**, *350*, 631–633; e) N. C. Seeman, *Acc. Chem. Res.* **1997**, *30*, 357–363.
- [3] a) D. Bach, I. R. Miller, *Biochim. Biophys. Acta* **1966**, *114*, 311–325; b) I. R. Miller, D. Bach, *Biopolymers* **1968**, *6*, 169–179; c) P. L. Felgner, T. R. Gadek, M. Holm, R. Roman, H. W. Chan, M. Wenz, J. P. Northrop, G. M. Ringold, M. Danielsen *Proc. Natl. Acad. Sci. USA* **1987**, *84*, 7413; d) H. J. Vollenweider, J. M. Sogo, T. H. Koller *Proc. Natl. Acad. Sci. USA* **1975**, *72*, 83–87.
- [4] G. Van Tendeloo, J. Van Landuyt, S. Amelinckx in *Fullerenes: Recent Advances in the Chemistry and Physics of Fullerenes and Related Materials* (Eds.: K. M. Kadish, R. S. Ruoff), Electrochemical Society, Pennington, NJ, **1994**, pp. 498–513.

- [5] A. S. Buotrine, H. Tokuyama, M. Takasugi, H. Isobe, E. Nakamura, C. Hélène; *Angew. Chem.* **1994**, *106*, 2526–2529; *Angew. Chem. Int. Ed. Engl.* **1994**, *33*, 2462–2465.
- [6] a) M. Maggini, G. Scorrano, M. Prato, *J. Am. Chem. Soc.* **1993**, *115*, 9798–9799; b) R. Bullard-Dillard, K. E. Creek, W. S. Scrivens, J. M. Tour, J. M., *Bioorg. Chem.* **1996**, *24*, 376–385.
- [7] A. W. Jowdy, *Carol. J. Pharm.* **1952**, *33*, 465.
- [8] The circumference of the DNA was calculated by multiplying the number of base pairs (5386) with the distance between base pairs for B-form DNA (0.34 nm). The circumference was then divided by  $\pi$  to obtain the diameter of the B-form DNA in the plasmid. See: D. Freifelder, R. DeWitt, *Gene* **1977**, *1*, 385.
- [9] C. K. Mathews, K. E. van Holde *Biochemistry*, 1st ed., Benjamin/Cummings, New York, **1990**, pp. 1003–1007.
- [10] J. K. Lindsay, C. R. Hauser *J. Org. Chem.* **1957**, *22*, 355.

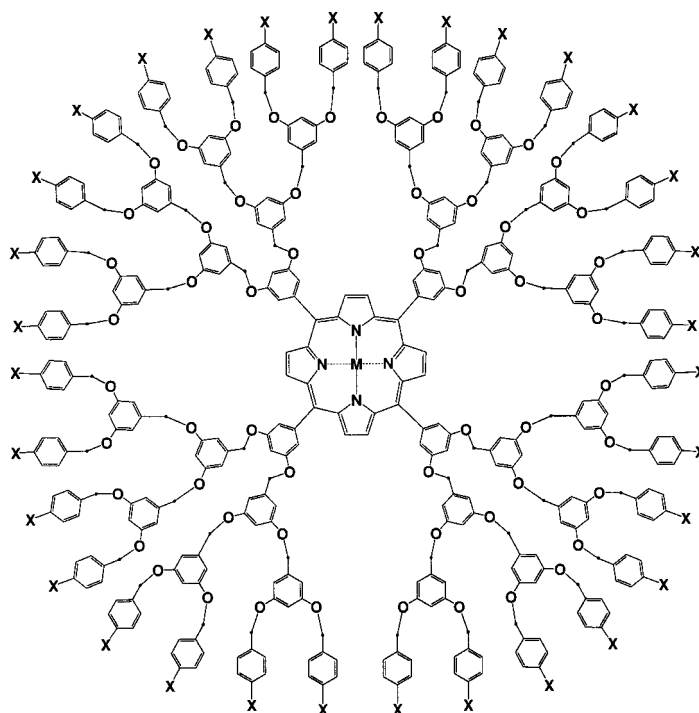
## Electrostatic Assembly of Dendrimer Electrolytes: Negatively and Positively Charged Dendrimer Porphyrins\*\*

Nobuyuki Tomioka, Daisuke Takasu, Toshie Takahashi, and Takuzo Aida\*

Dendrimers are nanosized hyperbranched macromolecules with well-defined three-dimensional shapes<sup>[1]</sup> and are potential building blocks for the construction of organized functional materials with nanometric precision. Therefore, it is important to develop a synthetic method that enables controlled spatial arrangement of functional dendrimers. Recently some conelike dendrimers (dendrons) were reported to self-assemble with the aid of van der Waals, hydrogen-bonding, and metal-ligating interactions into superstructures with spherical, disklike, and other configurations.<sup>[2, 3]</sup> Here we present results of the first study on electrostatic assembly of dendrimer electrolytes.<sup>[4]</sup> For this purpose we utilized negatively and positively charged dendrimers that contain within their frameworks a fluorescence probe in the form of a porphyrin (either as a free base or as a zinc complex).

We previously reported the convergent synthesis<sup>[5]</sup> of a negatively charged, water-soluble dendrimer zinc porphyrin (32[–]DPZn) with 32 carboxylate ion functionalities on its exterior surface.<sup>[6]</sup> This photofunctional macromolecule consists of a four-layered aryl ether dendrimer framework, and is expected to adopt a spherical conformation with an estimated

diameter of 4–5 nm.<sup>[7]</sup> We have now synthesized from 32[HO<sub>2</sub>C]DPZn<sup>[6]</sup> a positively charged dendrimeric zinc porphyrin, 32[+]DPZn, with 32 ammonium ion functionalities on its periphery.



32[MeO <sub>2</sub> C]DPH <sub>2</sub> :	X = CO <sub>2</sub> Me, M = H <sub>2</sub>
32[MeO <sub>2</sub> C]DPZn:	X = CO <sub>2</sub> Me, M = Zn
32[HO <sub>2</sub> C]DPH <sub>2</sub> :	X = CO <sub>2</sub> H, M = H <sub>2</sub>
32[HO <sub>2</sub> C]DPZn:	X = CO <sub>2</sub> H, M = Zn
32[–]DPH <sub>2</sub> :	X = CO <sub>2</sub> <sup>–</sup> K <sup>+</sup> , M = H <sub>2</sub>
32[–]DPZn:	X = CO <sub>2</sub> <sup>–</sup> K <sup>+</sup> , M = Zn
32[Me <sub>2</sub> N]DPZn:	X = CONH(CH <sub>2</sub> ) <sub>2</sub> NMe <sub>2</sub> , M = Zn
32[+]DPZn:	X = CONH(CH <sub>2</sub> ) <sub>2</sub> N <sup>+</sup> Me <sub>3</sub> Cl <sup>–</sup> , M = Zn

To investigate the possibility of electrostatic assembly between the negatively and positively charged dendrimer electrolytes 32[–]DPH<sub>2</sub> (free-base porphyrin) and 32[+]DPZn, the transmittance at 500 nm<sup>[8]</sup> was monitored when solutions of the two in phosphate buffer (pH 6.9, 1.5 μM) were mixed at 20 °C. As shown in Figure 1, the transmittance of the solution was highly dependent upon the molar ratio of the two dendrimer electrolytes, and it dropped sharply when the two concentrations were nearly equal. Fluorescence microscopy of a 100 μM phosphate buffer solution of either 32[–]DPZn (Figure 2a) or 32[+]DPZn excited at 400–440 nm (Soret bands) revealed strong, homogeneous emission from the entire solution. On the other hand, when the two solutions were mixed in an equimolar ratio ([32[–]DPZn]:[32[+]DPZn] = 1:1) the microscope image became dark, and large fluorescent aggregates (10–20 μm) were observed (Figure 2b). If this mixture was allowed to stand for a day at room temperature, the aggregates continued to grow and then precipitated out of the solution. If either 32[–]DPZn or 32[+]DPZn was present in excess, no aggregate formation was detected. Thus, 32[–]DPZn and

[\*] Prof. Dr. T. Aida, N. Tomioka, D. Takasu  
Precursory Research for Embryonic Science and Technology (PRESTO), JST  
and  
Department of Chemistry and Biotechnology  
Graduate School of Engineering, The University of Tokyo  
7-3-1 Hongo, Bunkyo-ku, Tokyo 113-8656 (Japan)  
Fax: (+81) 3-5802-3363  
E-mail: aida@macro.t.u-tokyo.ac.jp  
Dr. T. Takahashi<sup>[+]</sup>  
Department of Biochemistry and Molecular Biology  
Graduate School of Medicine, The University of Tokyo (Japan)

[+] Mass spectra

[\*\*] Supporting information for this article is available on the WWW under <http://www.wiley-vch.de/home/angewandte/> or from the author.